



# Targeting Superficial or Nodular Basal Cell Carcinoma with Topically Formulated Small Molecule Inhibitor of Smoothened

## Citation

Tang, Tracy, Jean Y. Tang, Dongwei Li, Mike Reich, Christopher A. Callahan, Ling Fu, Robert L. Yauch, et al. 2011. Targeting Superficial or Nodular Basal Cell Carcinoma with Topically Formulated Small Molecule Inhibitor of Smoothened. *Clinical Cancer Research* 17, no. 10: 3378–3387.

## Published Version

doi:10.1158/1078-0432.CCR-10-3370

## Permanent link

<http://nrs.harvard.edu/urn-3:HUL.InstRepos:12992309>

## Terms of Use

This article was downloaded from Harvard University's DASH repository, and is made available under the terms and conditions applicable to Open Access Policy Articles, as set forth at <http://nrs.harvard.edu/urn-3:HUL.InstRepos:dash.current.terms-of-use#OAP>

## Share Your Story

The Harvard community has made this article openly available.  
Please share how this access benefits you. [Submit a story](#).

[Accessibility](#)

Published in final edited form as:

*Clin Cancer Res.* 2011 May 15; 17(10): 3378–3387. doi:10.1158/1078-0432.CCR-10-3370.

## Targeting Superficial or Nodular Basal Cell Carcinoma with Topically Formulated Small Molecule Inhibitor of Smoothed

Tracy Tang<sup>1,\*</sup>, Jean Y. Tang<sup>2,\*</sup>, Dongwei Li<sup>1</sup>, Mike Reich<sup>1</sup>, Christopher A. Callahan<sup>1</sup>, Ling Fu<sup>1</sup>, Robert L. Yauch<sup>1</sup>, Frank Wong<sup>3</sup>, Karen Kotkow<sup>3,4</sup>, Kris Chang<sup>5</sup>, Elana Shpall<sup>5</sup>, Angela Wu<sup>5</sup>, Lee L. Rubin<sup>4</sup>, James C Marsters Jr<sup>1</sup>, Ervin H. Epstein Jr<sup>5</sup>, Ivor Caro<sup>1</sup>, and Frederic J. de Sauvage<sup>1</sup>

<sup>1</sup>Genentech, One DNA Way, South San Francisco, CA 94080, USA

<sup>2</sup>Stanford University School of Medicine, 450 Broadway Street, Redwood City, CA 94063, USA

<sup>3</sup>Curis, 45 Moulton Street, Cambridge, MA 02138, USA

<sup>4</sup>Translational Medicine at Harvard University, Massachusetts Hall, Cambridge, MA 02138-3800

<sup>5</sup>Children's Hospital Oakland Research Institute, 5700 Martin Luther King Jr. Way, Oakland, CA 94609, USA

### Abstract

Inappropriate activation of the Hedgehog (Hh) signaling pathway in skin is critical for the development of basal cell carcinomas (BCCs). We have investigated the anti-BCC efficacy of topically-applied CUR61414, an inhibitor of the Hedgehog signal transduction molecule Smoothed. In mice, topical CUR61414 significantly inhibited skin Hh signaling, blocked the induction of hair follicle anagen, and shrank existing BCCs. However, we observed no clinical activity of this formulation in human superficial or nodular BCCs in a phase I clinical study. Our data highlight some of the challenges of translating preclinical experience into successful human results for a topical anti-cancer agent.

### Introduction

The Hedgehog (Hh) signaling pathway, which is active during embryonic development (1), is down-regulated in most normal adult tissues. However, aberrant activation of Hh signaling due to mutations in genes encoding signaling pathway components underlies most, if not all, human basal cell carcinomas (BCC), whether arising sporadically or in patients with the heritable basal cell nevus (Gorlin) syndrome (2); (3–6).

BCCs commonly contain mutations that inactivate the Patched 1 (PTCH1) receptor (4) or constitutively activate the Smoothed (SMO) receptor (7, 8). Both have the same functional consequence - the uncontrolled activation of the Hh signaling pathway independent of the ligand. Activation of the Hh pathway in nearly all human BCCs (9); (10) is indicated by increased expression of Hh target genes such as the transcription factor, glioma-associated oncogene homolog 1 (*GLI1*), and *PTCH1*, thus suggesting that this is a causal event in tumor initiation. Additional confirmation of the importance of this pathway in BCC was provided by studies of genetically engineered mice, which showed that BCC-

Correspondence should be addressed to F.J.d.S. (sauvage@gene.com) and EE (eepstein@chori.org).

\*These authors contributed equally to this work.

like lesions arise following the introduction of similar genetic perturbations that constitutively activate the Hh signaling pathway (11); (12); (13); (14); (7).

This direct link between the observed genetic mutations and the development of BCC lesions suggests that the development of molecules acting at the level of or downstream of SMO could effectively treat various types of BCCs. A proof of concept for the treatment of locally advanced and metastatic BCC has been provided in the clinic with GDC-0449, an orally available Hh pathway inhibitor acting at the level of SMO (15). However, a topical non-systemic Hh pathway inhibitor would be preferable for the treatment of localized BCCs as it could minimize any possible systemic side effects caused by generalized inhibition of Hedgehog signaling. Current treatments for superficial or nodular BCC include surgical excision, electrodesiccation and curettage, cryosurgery, and topical chemotherapies such as 5-fluorouracil and imiquimod. Scarring following surgical interventions and significant local skin reactions and limited efficacy restrict the use of the existing topical treatments, particularly in nodular BCC, and indicate the need for a new topical agent that has acceptable efficacy and is well tolerated.

CUR61414 is a small-molecule member of the aminoproline class of compounds that was identified in a high throughput screen for inhibitors of the Hh signaling pathway (16). Williams *et al.* demonstrated the potential therapeutic effectiveness of CUR61414 in *in vitro* murine models by using an embryonic *Ptch1*+/- skin explant assay in the presence of recombinant sonic hedgehog or adult *Ptch1*+/- skin with UV-induced microscopic BCCs. Like GDC-0449, CUR61414 acts downstream of the defective PTCH1 through antagonism of SMO (16).

Here we demonstrate that a topical formulation of CUR61414 can down-regulate *Gli-1* expression in normal mouse skin in an *in vivo* depilatory model and can cause significant tumor regression in a genetically engineered model of BCC. In addition, the safety, tolerability, and efficacy are reported for a phase I, double-blinded, randomized, placebo-controlled, multicenter study of CUR61414.

## Results

### Epidermal and dermal drug deposition and penetration in human skin

We first studied topically applied CUR61414 in an *in vitro* human abdominal cadaver skin percutaneous absorption assay. We formulated a cream base containing increasing concentrations of CUR61414 (1–4% w/w) spiked with tracer levels of <sup>14</sup>C-labeled CUR61414 (1.0 µCi/3.2 mg formulation dose). Following 24-hour exposure, the quantity of radioactivity in stratum corneum, epidermis, dermis, and receptor fluid samples indicated that both the epidermal drug deposition and the skin penetration were enhanced by increasing the CUR61414 concentration from 1% to 4% in the cream formulations (Table 1). Six to eleven percent and two to five percent of the applied doses were absorbed in the epidermis and dermis layers, respectively.

### Topical CUR61414 represses *Gli-1* expression in normal mouse skin in a depilatory model

To evaluate the ability of topical formulations of CUR61414 to repress Hedgehog responsive cells found at the base of hair follicles in normal skin (17); (18), we established and optimized a depilatory mouse model. The hair follicles in 7-week old *C57BL/6* mice are naturally synchronized in the telogen phase of the hair follicle cycle (Muller-Rover S *et al.*, 2001), and the onset of anagen, a process accompanied by Hh signaling activation, does not occur until 12 weeks of age. Chemical depilation with potassium thioglycolate (Nair) disrupts disulfide bonds, thus damaging hair follicles at the deep root sheath (19). This damage activates Hh signaling and hence induces the telogen hair follicles in 7-week old

mice to undergo anagen. The regeneration of hair follicle depends on the reactivation of follicle growth by the proliferation of the hair follicle stem cells at the onset of anagen phase, and Hh has been shown to act as an anagen-inducing signal (20); (21). Time course analysis of *Gli1* mRNA levels in skin following hair removal by a combination of shaving and Nair application was first performed to determine the magnitude and duration of Hh pathway activation in response to hair follicle damage (Figure 1a). Nair-induced depilation significantly elevated *Gli1* expression by day 4 (data not shown and Figure 1a), and this increase in *Gli1* expression was maintained through day 7.

To determine whether CUR61414 can block Hh pathway activation in this model, we first applied two doses of cream containing 1–3% CUR61414 (Figure 1b). Two percent CUR61414 caused maximal repression of *Gli1* expression. Furthermore, application of 2% CUR61414 twice daily over 3 days was more effective than once daily application (7-fold vs 3-fold *Gli1* down-regulation) (Figure 1c).

### Topical CUR61414 decreases Hh signaling and shrinks murine BCCs

We next tested the *in vivo* effects of topical CUR61414 on murine BCCs. After treatment with tamoxifen at 6 weeks of age and exposure to 4Gy of IR at 8 weeks of age, *Ptch1*<sup>+/-</sup> *K14-CreER2 p53 fl/fl* mice develop multiple visible nodular BCC tumors starting at 5–6 months of age (Epstein lab, manuscript in preparation). These murine BCCs histologically resemble nodular human BCCs (Figure 2a). Like BCCs in *Ptch1*<sup>+/-</sup> *p53* wild type mice (11) the tumors have a high proliferation index as measured by expression of Ki67 and express basal cell markers - keratins 14 and 17 (Figure 2a) - but not suprabasilar differentiation markers - keratin 10 (Figure 2a). These BCC tumors responded dramatically to topically applied CUR61414. While placebo-treated BCCs increased on average by 40% in size (as measured by tumor diameter) and none shrank during the course of the study, all CUR61414-treated BCCs decreased by an average of 60% ( $p < 0.0001$ ) (Figure 2b). Two of 10 CUR61414-treated tumors regressed completely, and the others regressed partially (>50% decrease). Decreased tumor size could be detected within as few as 6 days of treatment. Tumor size decrease was paralleled by a significant reduction of *Gli1* expression in CUR61414-treated BCCs compared to placebo-treated tumors ( $p = 0.011$ ) (Figure 2c).

Topical application of CUR61414 significantly reduced tumor proliferation as measured by Ki67 staining (Figure 2a; Figure 2d,  $p = 0.034$ ) but, unlike in the studies of Williams *et al.* (16), did not induce significant apoptosis as measured by cleaved-caspase 3 (data not shown). The lack of apoptosis in our model could be due to the absence of p53, although HhAntag treatment appears to increase apoptosis in *Ptch1*<sup>+/-</sup> *p53*<sup>-/-</sup> murine medulloblastomas (22). CUR61414 also caused tumor necrosis (Figure 2a) and, after 30 days of application, prominent differentiation of tumor cells as indicated by the development of large, keratin filled cysts (Figure 2a). Cysts developed in most (67%) CUR61414-treated BCCs compared to 18% in placebo-treated BCCs (Figure 2e,  $p = 0.02$ ), and cysts in both treatment groups expressed abundant keratins 14 and 17, but little keratin 10 (Figure 2a). These data suggest that CUR61414 induced cysts may be derived from BCC tumor cells or from hair follicles (23) and hence possibly indirectly from follicular stem cells (Wang and Epstein, Cancer Cell, in press). The cells lining the cysts also have low Ki67 staining. Our data suggest that topical CUR61414 reduces murine BCCs by decreasing tumor proliferation as measured by Ki67 and/or inducing follicular differentiation. These encouraging preclinical data prompted initiation of clinical testing.

### Clinical experience with CUR61414 in human BCCs

A Phase I, double-blind randomized, placebo-controlled, multicenter study (clinical trial ID THA3435g) was initiated to evaluate, as the primary objective, the safety and tolerability of

a multidose regimen of CUR61414 (0.09%, 0.35%, 1.1% and 3.1%) applied topically to human superficial or nodular BCCs for up to 28 days (Figure 3a). Between May 2005 and June 2006, a total of 42 patients were enrolled from seven sites within the United States (34 patients in the dose-escalation and MTD expansion segments of the study - 29 patients were randomized to active study drug and 5 to placebo; 8 patients in the PD segment - 6 randomized to active drug and 2 to placebo). No serious adverse events (SAEs) were reported, even at the highest dose tested of 3.1%. Of the adverse events (AEs) reported, the majority were skin-related and of mild severity, with one case of severe skin erythema in a subject treated at the highest dose.

A secondary objective was to assess clinical activity as determined by the percent of tumors with complete clearance (defined by clinical and histopathologic clearance) after 28 days of CUR61414 treatment compared to placebo. All target tumors were excised at Day 42. None of the subjects had complete clearance of their target BCC as defined by complete clinical and histopathologic clearance. However 2 subjects had histopathologic clearance with CUR61414 - one subject with a nodular BCC treated with 0.35% cream and the other subject with a superficial BCC treated with 3.1% cream.

We conducted a separate pharmacodynamic study in which we analyzed *GLII* mRNA levels in nodular BCCs on 8 patients before and after treatment with CUR61414 twice daily for 3.5 days (Figure 3b). This treatment failed to reduce *GLII* expression. Similarly, we found no significant changes in gene expression of three other Hedgehog transcriptional target genes (*GLI2*, *PTCH*, and *PTCH2*) further suggesting a lack of Hh-pathway modulation (data not shown). Consistent with the qPCR results, isotopic *GLII* and *PTCH1* in situ hybridization (ISH) showed no consistent reduction in *GLII* or *PTCH1* transcripts following drug treatment (Supplementary Tables 1 and 2), and both *GLII* and *PTCH1* transcript levels remained high in the superficial regions of the CUR61414-treated BCC tumors - the regions closer to the site of the topical treatment - and were comparable to the levels detected in the deeper layer of the biopsies (Figure 3c; Supplementary Tables 1 and 2).

CUR61414 treatment had little or no effect on the proliferation of BCC tumor cells as judged by Ki-67 staining (Supplementary Table 3). Likewise, IHC for cleaved caspase-3 revealed little or no impact of CUR61414 treatment on tumor cell apoptosis (Supplementary Table 4). Similar Ki-67 or cleaved caspase-3 level was observed between superficial and deep portions of tumors with drug treatment.

## Discussion

We have found that topical CUR61414 can down-regulate *Gli-1* expression in normal mouse skin in an *in vivo* depilatory model and can cause significant tumor regression in a genetically engineered model of BCC.

The development of a mouse depilatory model described here offered a controlled system where we could synchronize the hair cycle and reliably monitor drug-induced changes in *Gli1* mRNA levels. We used this model to rapidly screen multiple topical formulations of CUR61414 and to test various dosing regimens with a sufficiently large number of animals per group for statistical analysis.

We and others have shown amply that *Ptch1*<sup>+/-</sup> mice are susceptible to radiation-induced BCC tumor formation following cesium-137 irradiation (11, 24). Combining *Ptch* heterozygosity with keratin 14-specific deletion of p53 accelerates the rate of BCC tumor formation, avoids the early development of medulloblastomas that occurs in *Ptch*<sup>+/-</sup> *p53*<sup>-/-</sup> mice, and allows the generation of multiple visible BCCs that can be treated and monitored readily. PK analysis of drug concentrations in the plasma collected at the end of

the study showed negligible levels of systemic drug exposure (data not shown), and we could detect the effect of topical CUR61414 on *Gli1* transcript levels and tumor growth specifically in the drug-treated BCCs but not on untreated BCCs in the same mouse.

Genetically engineered mouse models of cancers offer powerful tools to test the activity of potential therapeutic agents (25). Nonetheless, the strong anti-SMO and anti-BCC efficacy of topical CUR61414 in the mice was inconsistent with its lack of efficacy on human tumors. In contrast to the murine studies, quantitative RT-PCR and isotopic *in situ* hybridization analysis of the human BCC lesions before and after drug treatment showed unchanged *GLII* expression, indicating lack of exposure. Consequently, CUR61414 did not achieve the secondary clinical activity endpoint of the Phase I study – there was no complete clinical and histopathologic clearance. This disparity contrasts with the similar anti-BCC efficacy of oral celecoxib in mice and humans (26) and indicates that differences between mouse and human in topical efficacy may exceed those of oral agents.

The lack of clinical efficacy and the failure of *topical* CUR61414 to down-regulate *GLII* in human BCCs is likely due to differential potency of the drug on human vs mouse SMO and/or inadequate drug concentrations in the BCCs due to low penetration or rapid clearance. CUR61414 is 7.5 fold more potent on mouse than human SMO at inhibiting Hh signaling activation in *in vitro* Gli-luciferase assays (IC<sub>50</sub> of 0.2μM in murine S12 cells vs. IC<sub>50</sub> of 1.5μM in human HEPM cells). This difference in potency could provide a simple explanation for the disparity we observed between mouse and human BCCs. However, when applied at the highest dose of 3.1%, the estimated effective concentration of CUR61414 at the target site is 75 times in excess of the IC<sub>50</sub>, 112μM based on 2% percutaneous absorption (Table 1). It is therefore likely that CUR61414 absorption in human BCCs is significantly lower than that in the human abdominal cadaver skin used in the percutaneous absorption.

We have developed other Hh inhibitors that are 10 to 100 fold more potent than CUR61414 as measured by IC<sub>50</sub>. The significant efficacy of an unrelated Hh pathway inhibitor, GDC-0449, delivered orally in patients with locally advanced and metastatic BCCs (15), illustrates the scientific validity of the target. In the future, new models to test human percutaneous absorption beyond Franz chamber testing will be needed to more effectively predict the clinical outcome for topically formulated applications.

## Materials & Methods

### Murine Studies

**Depilatory model**—Male mice (Charles River Laboratories, Hollister, CA), 7–8 weeks of age, at which time the hair follicles all are in telogen phase, and 25–30 grams in body weight, were used in the study following 2 days of acclimation. Only animals that appeared to be healthy and that were free of obvious abnormalities were used for the study. Mice, singly housed during study, were shaved on the dorsal shoulder area, a site difficult for the mouse to lick, and then treated with the depilatory Nair (Church & Dwight Co., Inc.; active ingredient: potassium thioglycolate), for 4 minutes before washing off to induce the hair cycle. Four or five days later, vehicle or drug-containing cream was applied to the depilated areas (~0.5 cm<sup>2</sup>). During topical application, mice were under anesthesia.

**Gene expression analysis by quantitative PCR**—Mouse skin and BCC samples were homogenized with Polytron homogenizer for 30sec -1min at speed 6. Total RNA was isolated from the homogenates (Rneasy Fibrous Midi Kit, Qiagen). RNA samples were DNase-treated (Dnase Kit, Invitrogen), and final RNA concentrations were determined at OD<sub>260</sub>. 100ng of RNA was used per well in Taqman quantitative qPCR. Relative mRNA



levels were expressed as  $[2^{-(\text{test gene Ct value} - \text{reference gene Ct value})}] \times 1000$ . The relative *Gli-1* mRNA levels were calculated based on normalization to the house keeping gene *Rpl19*.

***Ptch1*<sup>+/-</sup> *K14CreER p53 fl/fl* mice and in vivo efficacy study**—We have used BCC-susceptible, *Ptch1*<sup>+/-</sup> *K14Cre-ER2 p53 fl/fl* mice as a model for testing small molecule inhibitors of the Hh pathway. These were generated by breeding mice with the *K14-Cre-ER* transgene (27) and mice with a floxed *p53* allele (28) with *Ptch1*<sup>+/-</sup> mice (29). Mice were treated at 6 weeks of age with 100μg/day of tamoxifen administered intraperitoneally for three consecutive days and at 8 weeks of age with 4-Gy ionizing radiation (IR), 160kV, using an X-ray source (RadSource RS2000 irradiator) to induce BCC formation by 5 months of age. CUR61414 (3.5% wt/wt, formulated in a topical aqueous base cream) or placebo base cream was applied topically twice daily to BCCs on the dorsal skin 5 days a week for up to 42 days. A total of 9 mice with 20 tumors (less than 14mm diameter) were treated. Two mice had multiple BCCs that were distantly spaced and thus some BCCs were treated with CUR61414 and others on the same mouse with placebo. Three mice with closely spaced BCCs were treated with CUR61414 only, and four mice with tumors were treated with placebo only. In summary, 4 mice with 10 tumors (mean size 7.2 mm) were treated with placebo and 5 mice with 10 tumors (mean size 7.0 mm) were treated with CUR61414. The largest tumor diameter was measured thrice weekly by calipers. As per IACUC guidelines, mice with tumors exceeding 20mm in diameter were euthanized.

**β-gal staining and Immunohistochemistry**—Seven placebo-treated and six CUR61414-treated BCCs had enough BCC tumor material for immunohistochemistry and Ki67 analysis. *LacZ*-encoded bacterial β-galactosidase was detected by incubation of glutaraldehyde and formalin fixed tissue with X-gal and iron buffer solution using a β-gal staining set (Roche Applied Science, Indianapolis, IN) for 48 hours. Mouse tissues were fixed in 10% buffered formalin, embedded in paraffin, and cut into 5micron sections. Sections were deparaffinized in xylene and rehydrated through down grading alcohol. Antigen retrieval was carried out in Trilogy solution (Cell Marque, Rocklin, CA) by heating in a pressure cooker. Sections were blocked with 3% hydrogen peroxide, Avidin Biotin blocking system, and normal goat serum (Vector laboratories, Burlingame, CA) prior to incubation with various rabbit anti mouse polyclonal antibodies [K10 (1:500), K14 and K17 (1:2000) (Covance, Princeton state, NJ), caspase-3 (1:800) (Pharmingen, San Diego, CA) (overnight at 4°C), and Ki67 (1:400) (Thermo Scientific, Waltham, MA) (60 minutes at room temperature)] and control rabbit immunoglobulin (1:250). Biotinylated goat anti rabbit (Vector laboratories, Burlingame, CA) was used to detect the primary antibody and was followed by incubation with the Vectastain ABC kit (Vector laboratories, Burlingame, CA). Sections were visualized with liquid DAB and substrate chromogen system (Dako, Carpinteria, CA) and counterstained with hematoxylin.

**Statistical analysis**—Nonparametric t-tests (Mann-Whitney) were used to compare the difference in median values of *Gli1* mRNA levels and ordinal values of Ki67 staining (0:none to <25%, 1: 25–50%, 2: 50–74%, 3: >75% positivity), respectively. Chi-square tests were used to determine the difference in percentage of tumors with large cysts. All P values reported are two-sided. Graphpad Prism and STATA v10 were used for statistical software.

## Human Studies

***In vitro* human percutaneous absorption study**—This study was conducted using procedures described previously (30). The CUR61414 formulations (prepared by Dow Pharmaceutical Sciences) were comprised of CUR61414 (1–4% w/w), benzyl alcohol (0–3% w/w), propylene glycol (10.0% w/w), methylparaben (0.15% w/w), propylparaben

(0.05% w/w), emulsifying wax (15.0% w/w), 10% NaOH solution (q.s. pH 6.0), and purified water (q.s. to 100). Formulations were spiked with tracer levels (1.0  $\mu\text{Ci}$ /3.2 mg formulation dose) of (14C)-labeled CUR61414. Percutaneous absorption was evaluated using dermatomed human abdominal skin mounted on Bronaugh flow-through diffusion cells maintained at 32°C. The receptor fluid, PBS containing 0.1% sodium azide and 1.5% Oleth 20, was continuously pumped under the dermis at a flow rate of 1 ml/hr and collected in 6-hour intervals. A single dose (~5 mg formulation/cm<sup>2</sup>) was applied to the skin. Following 24-hour exposure, formulation residing on the skin surface was removed by wiping with two dry cotton swabs. The stratum corneum was removed from the epidermis with a single cellophane tape-strip and dissolved in 4ml tetrahydrofuran (THF). The remaining epidermis was then physically separated from the dermis and digested separately in 2N KOH. Quantity of radioactivity in the wipes, tape-strip, epidermis, dermis, and receptor fluid samples was determined using liquid scintillation counting techniques. Epidermal and dermal drug deposition as well as drug penetration were statistically evaluated by performing unpaired student's t-tests (significant differences between formulations are defined with a value of  $p < 0.05$ ).

**Clinical study**—A Phase I, double-blind randomized, placebo-controlled, multicenter study (conducted at 7 investigational sites in the United States) was designed to evaluate the safety and tolerability of a multidose regimen of CUR61414 topically applied to superficial or nodular BCCs. The study was reviewed and approved at each investigational site by institutional review boards in accordance with clinical guidelines. Patients with a single or multiple superficial or nodular BCC(s) who met the inclusion and exclusion criteria described in Supplemental Materials and Methods were eligible for study participation. All patients provided informed consent.

A single BCC lesion, confirmed by biopsy during screening (performed by the Principal Investigator or a sub-investigator who was a board-certified dermatologist), was targeted for treatment with the study drug (CUR61414 or placebo). Up to three BCCs per patient were biopsied at screening to select a single target BCC for treatment. The biopsy site of the targeted BCC was to be adequately healed (up to 14 days) prior to the initiation of treatment. Other (nontarget) BCCs that may have been present were not treated with the study drug. All treated lesions were completely excised to clear margins after the treatment and observation periods. During all study segments, the evaluating physician assessed safety and the appearance of the BCC lesion and performed general physical examinations of patients. For the dose-escalation and MTD expansion segments, the BCC was measured and documented by digital photography at screening and on Days 1, 8, 15, 22, 28, and 42.

Once the MTD was determined, enrollment began for the PD marker segment. A total of 8 subjects with a biopsy-confirmed nodular BCC were randomized in a 3:1 ratio (CUR61414 to placebo) to receive 3.1% CUR61414 topically applied twice daily [i.e., every 12 hours ( $\pm$  1 hour)] to the target BCC for 3.5 days, with the final (seventh) dose of study drug being applied the morning of Day 4. In addition to histopathologic confirmation of the BCC during the screening period, the biopsy sample was also used to determine the pre-treatment level of *GLII* expression. Treatment of the BCC consisted of topical application of a continuous thin film of study drug over the entire surface of the target BCC and margins.

Detailed information about the clinical protocol is described in Supplemental Materials and Methods.

## Supplementary Material

Refer to Web version on PubMed Central for supplementary material.



## Acknowledgments

We thank D. Metzger and P. Chambon their generous donations of the *K14-CreER2* mice and A. Berns for the *p53<sup>fl</sup>* mice used in the Epstein laboratory. This research was supported in part by a generous donation from the Michael J Rainen Family Foundation. Frank Wong, Karen Kotkow, and Lee L. Rubin were employees of Curis, Inc. during this work. Tracy Tang, Dongwei Li, Mike Reich, Christopher A. Callahan, Ling Fu, Robert L. Yauch, James C. Marsters Jr., Ivor Caro, and Frederic J. de Sauvage are employees of Genentech, Inc., a wholly owned subsidiary of Hoffmann-La Roche.

## References

- McMahon AP, Ingham PW, Tabin CJ. Developmental roles and clinical significance of hedgehog signaling. *Curr Top Dev Biol.* 2003; 53:1–114. [PubMed: 12509125]
- Epstein EH. Basal cell carcinomas: attack of the hedgehog. *Nat Rev Cancer.* 2008; 8:743–754. [PubMed: 18813320]
- Aszterbaum M, Rothman A, Johnson RL, et al. Identification of mutations in the human PATCHED gene in sporadic basal cell carcinomas and in patients with the basal cell nevus syndrome. *J Invest Dermatol.* 1998; 110:885–888. [PubMed: 9620294]
- Gailani MR, Stähle-Bäckdahl M, Leffell DJ, et al. The role of the human homologue of *Drosophila* patched in sporadic basal cell carcinomas. *Nat Genet.* 1996; 14:78–81. [PubMed: 8782823]
- Johnson RL, Rothman AL, Xie J, et al. Human homolog of patched, a candidate gene for the basal cell nevus syndrome. *Science.* 1996; 272:1668–1671. [PubMed: 8658145]
- Hahn H, Wicking C, Zaphiropoulos PG, et al. Mutations of the human homolog of *Drosophila* patched in the nevoid basal cell carcinoma syndrome. *Cell.* 1996; 85:841–851. [PubMed: 8681379]
- Xie J, Murone M, Luoh SM, et al. Activating Smoothed mutations in sporadic basal-cell carcinoma. *Nature.* 1998; 391:90–92. [PubMed: 9422511]
- Reifenberger J, Wolter M, Weber RG, et al. Missense mutations in SMOH in sporadic basal cell carcinomas of the skin and primitive neuroectodermal tumors of the central nervous system. *Cancer Res.* 1998; 58:1798–1803. [PubMed: 9581815]
- Dahmane N, Lee J, Robins P, Heller P, Ruiz i Altaba A. Activation of the transcription factor Gli1 and the Sonic hedgehog signalling pathway in skin tumours. *Nature.* 1997; 389:876–881. [PubMed: 9349822]
- Undén AB, Zaphiropoulos PG, Bruce K, oftgård R, Stähle-Bäckdahl M. Human patched (PTCH) mRNA is overexpressed consistently in tumor cells of both familial and sporadic basal cell carcinoma. *Cancer Res.* 1997; 57:2336–2340. [PubMed: 9192803]
- Aszterbaum M, Epstein J, Oro A, et al. Ultraviolet and ionizing radiation enhance the growth of BCCs and trichoblastomas in patched heterozygous knockout mice. *Nat Med.* 1999; 5:1285–1291. [PubMed: 10545995]
- Grachtchouk M, Mo R, Yu S, et al. Basal cell carcinomas in mice overexpressing Gli2 in skin. *Nat Genet.* 2000; 24:216–217. [PubMed: 10700170]
- Nilsson M, Undén AB, Krause D, et al. Induction of basal cell carcinomas and trichoepitheliomas in mice overexpressing GLI-1. *Proc Natl Acad Sci U S A.* 2000; 97:3438–3443. [PubMed: 10725363]
- Oro AE, Higgins KM, Hu Z, Bonifas JM, Epstein EH Jr, Scott MP. Basal cell carcinomas in mice overexpressing sonic hedgehog. *Science.* 1997; 276:817–821. [PubMed: 9115210]
- Von Hoff DD, LoRusso PM, Rudin CM, et al. Inhibition of the hedgehog pathway in advanced basal-cell carcinoma. *N Engl J Med.* 2009; 361:1164–1172. [PubMed: 19726763]
- Williams JA, Guicherit OM, Zaharian BI, et al. Identification of a small molecule inhibitor of the hedgehog signaling pathway: effects on basal cell carcinoma-like lesions. *Proc Natl Acad Sci U S A.* 2003; 100:4616–4621. [PubMed: 12679522]
- St-Jacques B, Dassule HR, Karavanova I, et al. Sonic hedgehog signaling is essential for hair development. *Curr Biol.* 1998; 8:1058–1068. [PubMed: 9768360]
- Oro AE, Higgins K. Hair cycle regulation of Hedgehog signal reception. *Dev Biol.* 2003; 255:238–248. [PubMed: 12648487]

19. Lee JN, Jee SH, Chan CC, Lo W, Dong CY, Lin SJ. The effects of depilatory agents as penetration enhancers on human stratum corneum structures. *J Invest Dermatol.* 2008; 128:2240–2247. [PubMed: 18401425]
20. Sato N, Leopold PL, Crystal RG. Induction of the hair growth phase in postnatal mice by localized transient expression of Sonic hedgehog. *J Clin Invest.* 1999; 104:855–864. [PubMed: 10510326]
21. Schneider MR, Schmidt-Ullrich R, R P. The hair follicle as a dynamic miniorgan. *Curr Biol.* 2009; 19:R132–R142. [PubMed: 19211055]
22. Romer JT, Kimura H, Magdaleno S, et al. Suppression of the Shh pathway using a small molecule inhibitor eliminates medulloblastoma in Ptc1(+/-)p53(-/-) mice. *Cancer Cell.* 2004; 6:229–240. [PubMed: 15380514]
23. Yoshikawa K, Katagata Y, Kondo S. Relative amounts of keratin 17 are higher than those of keratin 16 in hair-follicle-derived tumors in comparison with nonfollicular epithelial skin tumors. *J Invest Dermatol.* 1995; 104:396–400. [PubMed: 7532196]
24. Mancuso M, Pazzaglia S, Tanori M, et al. Basal cell carcinoma and its development: insights from radiation-induced tumors in Ptc1-deficient mice. *Cancer Res.* 2004; 64:934–941. [PubMed: 14871823]
25. Singh M, Lima A, Molina R, et al. Assessing therapeutic responses in Kras mutant cancers using genetically engineered mouse models. *Nat Biotechnol.* 2010; 28:585–593. [PubMed: 20495549]
26. Tang JY, Aszterbaum M, Athar M, et al. Basal cell carcinoma chemoprevention with nonsteroidal anti-inflammatory drugs in genetically predisposed PTCH1+/- humans and mice. *Cancer Prev Res (Phila).* 2010; 3:25–34. [PubMed: 20051370]
27. Metzger D, Li M, Chambon P. Targeted somatic mutagenesis in the mouse epidermis. *Methods Mol Biol.* 2005; 289:329–340. [PubMed: 15502196]
28. Jonkers J, Meuwissen R, van der Gulden H, Peterse H, van der Valk M, Berns A. Synergistic tumor suppressor activity of BRCA2 and p53 in a conditional mouse model for breast cancer. *Nat Genet.* 2001; 29:418–425. [PubMed: 11694875]
29. Goodrich LV, Milenković L, Higgins KM, Scott MP. Altered neural cell fates and medulloblastoma in mouse patched mutants. *Science.* 1997; 277:1109–1113. [PubMed: 9262482]
30. Skelly JP, Shah VP, Maibach HI, et al. FDA and AAPS Report of the Workshop on Principles and Practices of In Vitro Percutaneous Penetration Studies: Relevance to Bioavailability and Bioequivalence. *Pharm Res.* 1987; 4:265–267.

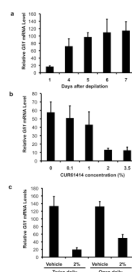


**Figure 1. Determination of the effective concentration of topical CUR61414 in a depilatory mouse model**

**a.** Time course of *Gli1* expression in normal skin after depilatory treatment. Thirty mice were shaved on the back shoulder area and then treated with the hair removal product Nair for 4 minutes to induce the hair cycle (day 0). Quantitative RT-PCR was performed to determine *Gli1* expression in the skin samples from mice sacrificed on indicated days (n=6 per time point). The relative *Gli1* expression was derived based on normalization to *Rpl19*. Error bars designate mean  $\pm$  SEM.

**b.** Mice (n=6 per group), shaved and Nair-treated, were treated 5 days post Nair with vehicle (2% benzyl alcohol) or 0.1%, 1%, 2%, or 3.5% CUR61414 wt/wt topically applied twice to the shaved area (16 hours apart) and sacrificed for skin tissues 4 hours after the second topical application. *Gli1* Ct values [measured as in (a)] were ~22–27.

**c.** Mice (n=6 per group), shaved and Nair-treated, were treated 4 days post Nair with 2% benzyl alcohol or 2% CUR61414 wt/wt topically applied to the shaved area twice a day (12 hours apart) for 3 days or once a day (24 hours apart) for 3 days. Skin tissues were harvested 12 hours after the sixth topical application or 24 hours after the third topical application and *Gli1* levels measured as in (a). *Gli1* Ct values were ~20–26.

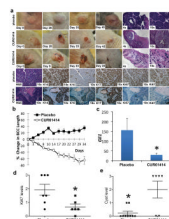


**Figure 2. CUR61414 mouse BCC Data**

**a.** Representative photos of BCC tumors treated with placebo or CUR61414. CUR61414 treatment leads to BCC regression and cysts or residual microscopic BCCs on histology. Cysts induced by CUR61414 strongly stain for K14 and K17 and have low staining for K10 similar to placebo-treated BCCs. Cells lining cysts also have low Ki67 staining.

**b.** BCC tumors treated with 3.5% CUR61414 wt/wt (N=10 tumors, 5 mice) vs. placebo cream (N=10 tumors, 4 mice) twice daily, 5 days per week. Mean and SEM (error bars) are shown.

**c.** Reduced *Gli1* mRNA levels (normalized to *Rpl19*) in tumors treated with CUR61414 (N=8) vs. placebo (N=5), Mean and SEM (error bars) are shown, \* p=0.011.

**d.** Reduced Ki67 staining in tumors treated with CUR61414 (N=7) vs. placebo (N=6), \* p=0.034. Ki67 levels were scored from 0 (none) to 3 (high) as detailed in Materials and Methods.

**e.** Percentage of tumors with large cysts, 67% of CUR61414 treated tumors (N=7) develop cysts on histology compared to 0% of placebo treated BCCs (N=6), \* p=0.009. A high number represents more cysts.

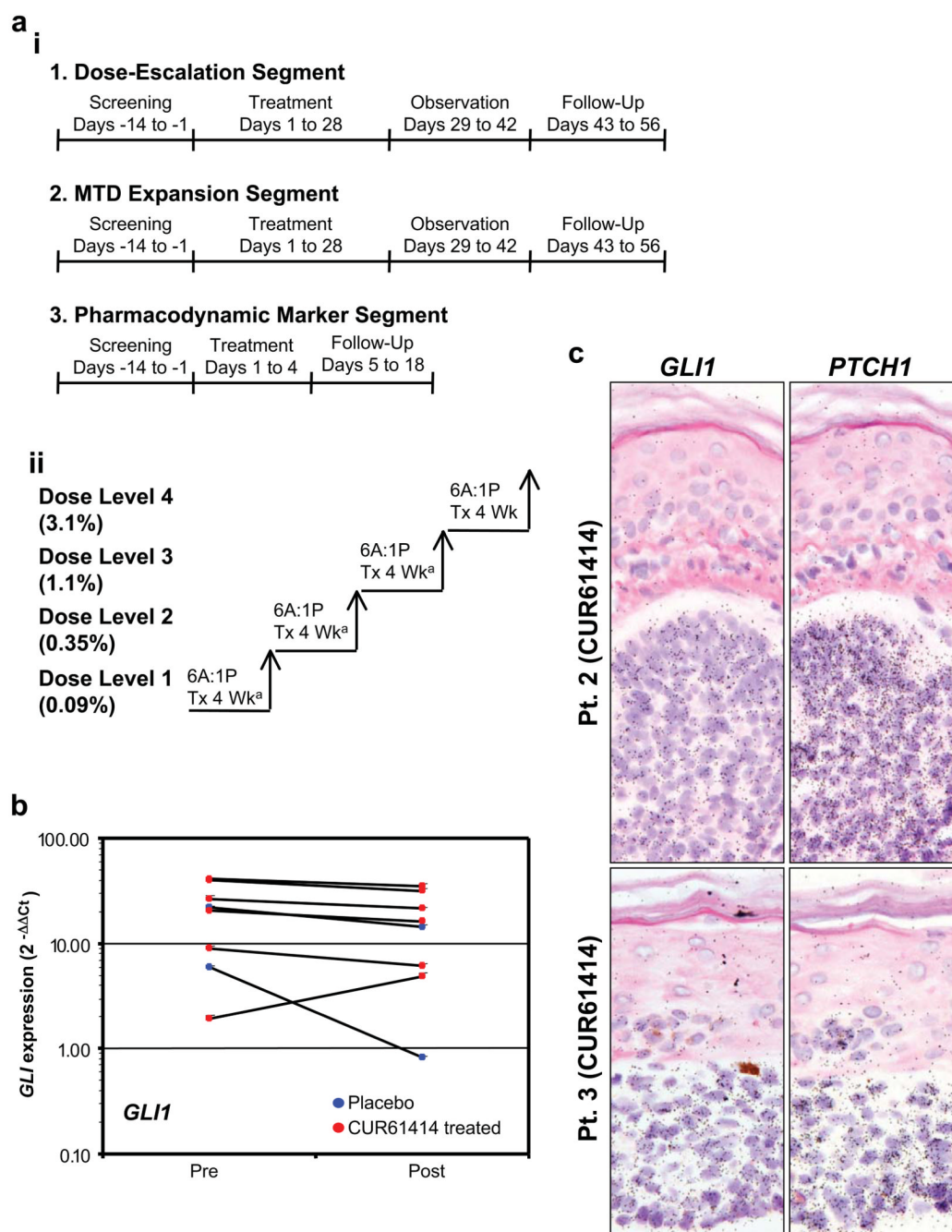


**Figure 3. CUR61414 Clinical Data**

**a. (i)** Three segments were included in this Phase I trial. The first was a dose-escalation segment, with four dose groups, for a total of 28 subjects (1). It consisted of four periods: screening (Day -14 to Day -1), treatment (Day 1 to Day 28), observation (Day 29 to Day 42), and follow-up (Day 43 to Day 56). The second segment was a maximum tolerated dose (MTD) expansion segment, consisting of the same four periods as the dose-escalation (2). The third was a pharmacodynamic (PD) marker segment consisted of three periods: screening (Day -14 to Day -1), treatment (Day 1 to Day 4), and follow-up (Day 5 to Day 18) (3). **(ii)** Segment 1 is a dose-escalation study (A = active; P = placebo; Tx = treatment). A low dose of 0.09% was chosen as the starting dose, with subsequent escalation to three

higher doses in a stepwise manner once all subjects in the dose level had been treated for 4 weeks and preliminary assessment of safety data indicated minimal or no toxicity. Concentrations in the higher dose levels were approximately three times the prior concentration, with the highest dose being 3.1%. One subject was randomized to receive placebo in each dose level. <sup>a</sup>All 7 subjects within a dose group completed the treatment period (4 weeks) prior to escalation to the next dose. For Dose Levels 1–3, if fewer than 2 subjects (i.e., 1 subject or no subjects) of the 6 actively treated subjects met the criteria for a DLT following assessment of preliminary safety data, then treatment at the next higher dose was initiated.

**b.** Summary of the pre-treatment and post-treatment *GLII* levels in the 8 patients enrolled in the PD marker segment. In an interim analysis, conducted after 8 patients were treated (2 patients randomized to placebo and 6 patients received study drug), the PD marker was evaluated by quantitative RT-PCR in the BCC lesion twice: prior to treatment and again in the excised lesion 4–6 hours following the last of seven doses on Day 4. A paired t-test was used to statistically compare pre- vs post-*GLII* levels within each treatment group (placebo and 3.1%) and a twosample t-test was used to compare the treatment differences between treatment groups. The observed “PD response” that was seen in one subject treated with placebo was likely due to differences in the cellular content of the post-treatment biopsy, as *SMO* expression was similarly decreased.

**c.** Representative images of *GLII* and *PTCH1* in situ hybridization on post-treatment BCC samples from two patients (Pt. 2 and Pt. 3) who received 7 doses of 3.1% CUR61414 topical application. A total of 11 matched pre- and post-treatment skin biopsies from four of the 8 PD patients (one placebo- and three CUR61414-treated) were found to contain suitable tumor material for immunohistochemical and in situ hybridization analyses. *GLII* and *PTCH1* levels (brown spots) in the superficial regions of the skin remained high and comparable to those detected in the deeper areas of the skin.



Table 1

a: Percutaneous Absorption of CUR61414 (% of applied dose *)						
CUR61414	Benzyl alcohol	Single Tape-strip	Epidermis	Dermis	Receptor	Dose Recovered
1%	0%	6.66±2.95	11.35±1.83	4.73±2.65	2.89±0.63	102.84±9.17
1%	1%	4.39±1.95	8.38±1.88	7.85±6.27	2.83±0.54	91.26±4.01
1%	2%	4.94±2.22	6.79±1.27	2.50±1.43	2.05±0.04	101.55±18.99
1%	3%	3.60±0.52	6.62±1.26	1.69±0.88	2.97±1.16	98.98±12.78
2%	0%	5.10±0.50	5.57±1.61	2.55±1.33	1.99±0.41	90.05±13.08
2%	1%	5.94±1.53	6.28±3.18	2.72±1.37	2.28±0.41	91.86±7.38
2%	2%	6.55±2.36	7.11±1.96	2.03±1.46	1.89±0.19	82.86±5.18
4%	0%	5.35±1.07	4.25±0.65	1.96±2.66	1.79±0.20	91.44±7.68
4%	1%	5.00±0.73	4.91±1.54	1.80±0.90	2.09±0.30	94.58±10.02
4%	2%	5.21±2.24	5.64±2.57	1.72±1.35	1.90±0.20	87.87±5.58

b: Percutaneous Absorption of CUR61414 (mass, µg *)				
CUR61414	Benzyl alcohol	Single Tape-strip	Epidermis	Receptor
1%	0%	2.13±0.94	3.63±0.58	1.51±0.85
1%	1%	1.62±0.61	2.73±0.57	2.05±1.70
1%	2%	1.58±0.71	2.17±0.41	0.80±0.46
1%	3%	1.15±0.17	2.12±0.40	0.54±0.28
2%	0%	3.26±0.32	3.57±1.03	1.63±0.85
2%	1%	3.80±0.98	4.02±2.04	1.74±0.88
2%	2%	4.19±1.51	4.55±1.25	1.30±0.93
4%	0%	6.85±1.37	5.44±0.83	2.51±3.41
4%	1%	6.40±0.93	6.28±1.97	2.30±1.16
4%	2%	6.66±2.87	7.22±3.29	2.20±1.73

\* mean±SD